BNL-101733-2014-TECH
RHIC/AP/78;BNL-101733-2013-IR

Closed Orbit Analysis for RHIC

J. Milutinovic

February 1989

Collider Accelerator Department
Brookhaven National Laboratory

U.S. Department of Energy
USDOE Office of Science (SC)

DISCLAIMER

AD/RHIC-AP-78

Closed Orbit Analysis for RHIC

J. Milutinovic and A.G. Ruggiero

BNL

February 21, 1989

Abstract

We examine the effects of four types of errors in the RHIC dipoles and quadrupoles on the on-momentum closed orbit in the machine. We use PATRIS both to handle statistically the effects of kick-modeled errors and to check the performance of the Fermilab correcting scheme in a framework of a more realistic modeling. On the basis of the accepted RMS values of the lattice errors, we conclude that in about 40% of all studied cases the lattice must be to some extent pre-corrected in the framework of the so-called "first turn around strategy," in order to get a closed orbit within the aperture limitations at all and, furthermore, for approximately 2/3 of the remaining cases we find that a single pass algorithm of the Fermilab scheme is not sufficient to bring closed orbit distortions down to acceptable levels. We have modified the scheme and have allowed repeated applications of the otherwise unchanged three bump method and in doing so we have been able to correct the orbit in a satisfactory manner. For orbit correctors, the maximum integrated kick strength that we have encountered was 1.7 kG.m, at the top magnetic rigidity $B\rho$ = 850 T.m.

Introduction

An accelerator lattice cannot be expected to be perfect and as an immediate consequence the same will be true for the closed orbit. Since more or less reliable assumptions can be made about realistic lattice errors, it is important to see how they translate into expected closed orbit distortions, and if the latter exceed acceptable levels to see how to correct them.

Among many possible sources of closed orbit distortions, we have selected four major types of lattice errors. They are the error in the integrated dipole field strength $\Delta(B\ell)/B\ell$, the axial tilt of the dipole $\Delta\theta$, and the lateral displacements of the quadrupole along the two transverse directions.

The RMS values of the lattice errors we have used are the following ones:

$\Delta(B\ell)/B\ell = 0.5 \times 10^{-3}$, $\Delta\theta = 10^{-3}$ radians,

Lateral quad displacements $\Delta_Q X = \Delta_Q Y = 0.25 \times 10^{-3}$ m.

A 2.5 σ cut was imposed on all distributions of random errors. Sextupoles were modeled as thin lenses, but in all other aspects they were assumed perfect. Higher order multipole errors have not been included yet. Orbit correctors were assumed to be thin lenses. Both beam position monitors and correctors were assumed ideal, i.e. perfectly aligned with the axis going through an ideally placed quadrupole and monitors were assumed to have a perfect sensitivity.

The tracking/analysis code PATRIS was used to handle the simulation and analysis of closed orbit distortions and furthermore to correct them. The lattice we used was RHIC88I, with β^* = 3m. The errors in this lattice cause bigger distortions of the closed orbit than the very same errors in the β^* = 6m case. Consequently, whatever remedy suffices in the β^* = 3m case it will also suffice in the β^* = 6m case.

The Results of Statistical Treatment of Closed Orbit Errors in the Kick Approximation

For the purpose of quick statistical treatment of the effects of magnet imperfections on the closed orbit, PATRIS employs an algorithm whose basic ingredients are given in the Courant-Snyder paper[1]. Some explanation on how PATRIS implements the ideas of this reference is also given in our technical note on the closed orbit analysis for the AGS Booster[2]. For this simple reason, details will not be repeated here. We would only mention that PATRIS runs over 21 independent distributions of random lattice errors and evaluates the appropriate orbit distortion RMS values at the end of each magnet. The effects of errors are evaluated in the kick approximation, with nonlinearities, including those coming from chromaticity correcting sextupoles, being disregarded. The only place where nonlinearities are (to some extent inconsistently) taken into account is evaluation of tune shifts and beta variations as a result of crossing of the sextupoles by a distorted closed orbit.

The resulting closed orbit distortions are displayed in Figure 1 and Figure 2, respectively for horizontal and vertical plane. One immediately observes how the RMS values of closed orbit distortions follow the local values of the relevant beta functions. In the insertions these RMS values can become quite large, around 50 mm or more. In regard to this, one must bear certain facts in mind. First, the values we display are RMS values, which means that even less desirable values of orbit distortions may appear in practice. Second, the effects of nonlinearities on the magnitudes of closed orbit distortions are disregarded, and various nonlinearities, once being included, certainly will not help. Third, no correctors are engaged at this stage, so one should not panic at these fairly large values of distortions.

The results of the effects of the sextupole crossing by a distorted closed orbit are given in Table 1. One will notice that 10 out of 21 distributions of random lattice errors produce unstable lattices when the sextupoles are taken into account, at the specified input RMS values of magnet imperfections (the value -1.0 in the output is meant to signal an instability). The remaining 11 distributions have produced pretty hefty beta variations and tune shifts. The bottom line displays the RMS values of the tabulated quantities. Again, the reader should keep in mind the fact that no orbit correction has been attempted in this simulation. Any successful correction will bring these large values down and will restore the stability of the lattice in the 10 worst cases.

The results from Table 1 have also been plotted. Vertical versus horizontal tune shift is plotted in Figure 3, whereas vertical versus horizontal $\Delta\beta/\beta$, evaluated at a horizontally focusing quad in the middle of an inner arc, is plotted in Figure 4.

The Results of Realistic Closed Orbit Modeling. The Performance of the Fermilab Correcting Scheme on RHIC

For a realistic closed orbit modeling, it is desirable to have a better scheme than that of a simple representation of lattice error effects by kicks. Furthermore, one would like to see what happens with closed orbit distortions once a certain well-defined sort of correction is implemented. Both goals have been attained in PATRIS, which on the one hand has the capabilities of simulating the lattice errors by incorporating them realistically into its 7 x 7 transfer matrix, and which on the other hand can correct the orbit by engaging the Fermilab correcting scheme, based on the so-called three bump method. The details of this scheme can be found elsewhere and will not be repeated here. The only thing we will emphasize here are placements of correctors. They are assumed to be BPM's at the same time and they have been placed beside focusing quadrupoles where the relevant beta function is large. Also, it is worthwhile to mention that in the arcs the orbit correctors at the same time appear to be adjacent to the chromaticity correcting sextupoles.

We started our analysis by assuming somewhat too stringent demands on acceptable lattice errors. All four types of errors were assumed to be at 10^{-4} levels in the appropriate units. We noticed that PATRIS always found a periodic solution for the perturbed lattice, but could not correct the distorted closed orbit down to acceptable levels (~ 1 mm) for a significant fraction of the 12 random error distributions we used [F1]. We attempted to cure this problem by introducing more correctors at additional locations, but improvements were almost negligible. We also attempted to correct the orbit with an overall scaling of evaluated corrector strengths, to see if we can undo a possible overcorrection/undercorrection, but no improvement resulted. Finally, we decided to abandon one basic assumption of the Fermilab correcting scheme: it is a single pass around, linear correcting algorithm. We made the necessary modifications and enabled PATRIS to repeat the correction several times if necessary. This action solved the problem; the second pass brought the orbit distortions down to acceptable levels. From that point we moved on to a more realistic set of lattice errors, given in the Introduction of this note.

As we have already mentioned, we had run 12 different random error distributions, at the RMS levels: $\Delta(B\ell)/B\ell = 0.5 \times 10^{-3}$, $\Delta\theta = 1.0 \times 10^{-3}$, with quadrupole lateral displacement 0.25×10^{-3} m in each plane, and with a 2.5 σ cut imposed on all random number distributions.

In five out of these twelve cases badly distorted closed orbits were found, but attempts to correct them resulted in unstable lattices. These instabilities showed up in various ways; in one case the code printed out det $|M - I| \sim 10^{-3}$, which indicated the proximity of an integer tune, and then stopped, in some other cases the code stopped and displayed the message "Tr M > 2" in one plane, and finally there were cases when the code crashed even before being able to evaluate the one-turn map and its linearization M and to conclude that the lattice was unstable [F2].

In the remaining seven cases the modified Fermilab scheme clearly worked well. Their results are displayed in Table 2. The first three cases in the table are called "good." We call them in this manner since the second correction sufficed. These three cases are followed by two cases we call "fair." This is because the results of the second correction are not too far from the levels which might be acceptable (~ 1mm, or a little bit over). The last two cases we call "poor." The reasons for this characterization should be obvious. First of all, after the second correction the maximum excursion of the closed orbit is still huge (i.e. beyond 10mm!). Furthermore, the improvement between the first and the second correction is only about a factor two. In addition to this, the quality of the first correction is very low in both cases; indeed, very sharp readjustments of kick strengths between the first and the second correction are the most significant indicators of this questionable initial efficiency [F3]. However, the second correction brings even these two poor cases in line with the others and the third correction is then sufficient.

We would also like to mention that the worst of all working examples (the last example in Table 2), behaved as a sort of average example in the twelve pilot runs with the RMS lattice error levels 10^{-4}, when all twelve sets of random errors generated a lattice whose stability was preserved in the process of orbit correction. For this reason, we have retained this example as a kind of "average" case out of twelve cases and have decided to use it to represent a succession of three corrections in Figures 5, 5a, 5b, 6, 6a, and 6b. Only one superperiod is shown since otherwise the figures would be too crammed for the effects of subsequent corrections to be discernable.

Finally, one should address two additional issues. The first one is the maximum corrector strength needed in the lattice. The second one is the ability of the hardware to readjust finely enough the kick strengths between the two subsequent corrections of the orbit.

The first issue is easily resolved by observing that since the kick strength $\delta\theta = \delta(B\ell)/B\rho$ it follows that each milliradian of $\delta\theta$ translates into the integrated strength $\delta(B\ell) = (10^{-3}\ B\rho)$ T.m = 8.5 kG.m at the top magnetic rigidity $B\rho = 850$ T.m. The maximum kick angle we picked up in the seven successful runs was 0.196 milliradians, which will then translate into a 1.7 kG.m demand on the correctors' maximum integrated strength.

To address the second issue, namely the hardware ability to make sufficiently precise readjustments between the two subsequent actions of the correcting algorithm, we call the reader's attention to Table 3. In this table we have displayed the kick strengths of the first 25 dipole correctors in each corrective pass, as evaluated by the modified algorithm of the Fermilab correcting scheme. The reader will notice the interesting fact that between the monitors number 7 and 16 the algorithm does not readjust the values of the kick strengths found in the first pass. This may seem bizzare at first glance, but this region is an insertion without sextupoles (and also without other nonlinearities in our simulation excercise) and one can show that the kick strengths evaluated by the Fermilab correcting scheme, for a given set of orbit distortions, in a region free from nonlinearities depend only on the elements of the linear transfer matrix in this region and not on anything outside the region. The presence of external nonlinearities will only degrade the quality of the correction inside the nonlinearity-free region, i.e. the corrected closed orbit will not shrink to zero, but the corrector strengths inside the region remain unaffected. However, the presence of nonlinearities does affect correction strengths in the regions with nonlinearities. Therefore, if one takes two cases, one with sextupoles on and another with sextupoles off, then a one-pass Fermilab correction will shrink the corrected closed orbit distortions to zero at every monitor/corrector if all of the sextupoles are off, and nowhere exactly to zero if some of the sextupoles are on. Furthermore, the two cases will have different kick strengths in the regions with sextupoles, but the same strengths in the nonlinearity-free regions.

From the foregoing it should also be obvious that the second and further passes must leave the correctors' strengths unchanged in nonlinearity-free regions while at the same time keeping readjusting other correctors to get better and better orbit in each subsequent pass. In a real RHIC, of course, the insertions will contain nonlinearities from sources other than the chromaticity correcting sextupoles and the modified Fermilab algorithm will therefore readjust the insertion correctors in each pass too. To come back to the issue in question, we analyze the amount of necessary readjustment between two subsequent passes. We notice that with the hardware ability to readjust the dipole correctors to an accuracy of 10^{-3} of the required maximum integrated corrector strength we can change the kick strength by approximately $0.2 \times 10^{-3} = 2 \times 10^{-4}$ milliradians. From Table 3 it is now obvious that the hardware will be capable of readjusting the kick strengths to move effectively from the second pass to the third one, which was enough in all our cases of successful orbit correction (i.e. seven out of twelve cases when the lattice was not made unstable by the very first correction). The 10^{-3} readjusting accuracy might be insufficient for a proper execution of the fourth correction, but an improvement of the hardware ability from a 10^{-3} to a 5×10^{-4} level will guarantee a feasibility of the fourth correction, if needed. Further studies will be necessary to determine if such a need might realistically arise, but our current conclusion is that three corrective passes should work well.

Conclusion

In our analysis of the closed orbit problem in RHIC, we have inevitably had to face the fact that this is by no means an easy machine to correct. Even at the very stringent 10^{-4} lattice error RMS values, the Fermilab scheme could not correct the orbit to acceptable levels, in a single pass. A multipass generalization of the correcting scheme, which we implemented in PATRIS, worked well at this level of errors but failed in 5 out of 12 cases when the lattice errors were allowed to assume more realistic RMS values. In these five "pathological" cases the lattice was still stable, the closed orbit was found by PATRIS but the first correction failed by producing an unstable lattice. Moreover, the uncorrected orbit was so grossly distorted that it exceeded physical aperture limitations in dozens if not hundreds of places in the lattice. Under such harsh but not unlikely circumstances, the beam would never make its first turn around in a real machine and there would be no orbit at all to correct.

The problem will have to be dealt with in the framework of the first turn around strategy. The orbit would then be already partially corrected (or pre-corrected) once the first turn around has been established, and at that point a multipass Fermilab algorithm will have worked. We are currently working in this direction, having two possible approaches or a combination thereof in mind. One is to invest more efforts in attempting to undo a possible overcorrection in the Fermilab scheme's first pass. The other is to try first to establish a reasonably behaved orbit at reduced strengths of chromaticity correcting sextupoles. Both approaches are promising but may encounter some limitations in a real machine. We plan to report our encouraging preliminary results in a separate technical note.

Finally, we would like to emphasize that the demands imposed by a multipass Fermilab scheme seem to be met by the previously proposed hardware.

Footnotes and References

F1 The problem existed only in the presence of nonlinearities (i.e. with sextupoles on). For a completely linear lattice the Fermilab scheme always corrects orbit distortions down to zero.

F2 There is a natural suspicion that these instabilities are the result of overcorrection (the lattice was rough but nevertheless stable in the absence of any correction). Further work is currently underway concerning various possibilities of preserving the stability of the lattice in the process of delivering the first correction. Preliminary results have been encouraging and more definite conclusions will be reported in a subsequent note.

F3 The extent of this readjustement is most reliably appreciated by observing the RMS values of kick strengths. Looking just at the maxima can be deceptive since some of the good distributions display even sign changes of the strongest kick in the lattice. Of course, in such cases the two extrema, from the two subsequent iterations, occur at two different correctors in the lattice.

Ref. 1 E. Courant & H. Snyder, Annals of Physics 3, 1 (1958).

Ref. 2 J. Milutinovic & A. G. Ruggiero, Closed Orbit Analysis for the AGS Booster, Booster Techical Note No. 107.

Tables

1. This table represents the tune shifts and the relative beta variations for the 21 runs over different distributions of random lattice errors, in the quick statistical mode of closed orbit analysis by PATRIS. The origin of these 21 shifts are the crossings of the sextupoles by the 21 different distorted on-momentum closed orbits. The lattice errors have been sufficiently large to make the lattice unstable in 10 out of these 21 cases. Such instabilities are characterized by the value -1.0 for these shifts in one or in both planes.

2. This table describes some characteristics of the seven cases where the distorted closed orbit has been successfully corrected. By "successful" we mean a correction capable of reducing orbit distortions to about one millimeter at the end of the corrective procedure. The first three distributions are commented as being "good." This is because the second iteration has been more than sufficient. The next two distributions are commented as "fair." This is because the second iteration nearly sufficed. The last two distributions are commented as "poor." This is because the results of the second iteration were still highly unsatisfactory. Furthermore, the kick strengths for the last two cases had undergone quite significant changes from the first to the second iteration (look at their RMS values, not at the extrema), which clearly indicates a very low quality of the first correction. However, after the second correction the scheme works fine.

3. This table displays how the kick strengths are being readjusted as the algorithm iterates. The total of five iterations are shown, even though there are no indications that so many iterations might ever be needed. The random error distribution is the worst among all that have been successfully corrected (i.e. the last item from Table 2). The kick strengths of the first 25 horizontal correctors starting from the middle of an inner arc are displayed. It is obvious that the algorithm does not readjust the kick strengths between the monitors number 7 and 16. They lie in an insertion which is (in our model) free from any nonlinearities.

Figure Captions

1. This figure represents the RMS values of the orbit distortions in the horizontal plane, for the 21 runs over different distributions of random lattice errors, in the quick statistical mode of closed orbit analysis by PATRIS. From the figure it is obvious how orbit distortions follow the local values of the horizontal beta function.

2. This figure represents the RMS values of the orbit distortions in the vertical plane, for the 21 runs over different distributions of random lattice errors, in the quick statistical mode of closed orbit analysis by PATRIS. From the figure it is obvious how orbit distortions follow the local values of the vertical beta function.

3. This figure represents the tune shifts for the 21 runs over different distributions of random lattice errors, in the quick statistical mode of closed orbit analysis by PATRIS. The origin of these shifts are the crossings of the sextupoles by the 21 different distorted on-momentum closed orbits. The lattice errors have been sufficiently large to make the lattice unstable in 10 out of these 21 cases. Hence, only eleven points, which correspond to the lattices stable in the presence of sextupoles, actually appear on this plot.

4. This figure represents the relative beta variations for the 21 runs over different distributions of random lattice errors, in the quick statistical mode of closed orbit analysis by PATRIS. The values are taken in the middle of an inner arc. The origin of these variations

are the crossings of the sextupoles by the 21 different distorted on-momentum closed orbits. The lattice errors have been sufficiently large to make the lattice unstable in 10 out of these 21 cases. Hence, only eleven points, which correspond to the lattices stable in the presence of sextupoles, actually appear on this plot.

5. This figure represents the orbit distortions found in the so-called "realistic closed orbit" modeling of PATRIS. The distribution is the worst one from the group of those found to be correctible. Besides the uncorrected orbit, the results of three subsequent corrections are shown. The distortions in this figure are those in the horizontal plane. One full superperiod is shown. The same situation is also represented in Figures 5a and 5b.

5a. This figure represents the same situation as Figure 5, but with the third correction omitted for a better discernability.

5b. This figure represents the same situation as Figure 5, but with the uncorrected orbit omitted and at a different scale for a better discernability.

6. This figure represents the same as Figure 5, but this time for the vertical plane. Figures 6a and 6b are added, in the same manner as Figures 5a and 5b in the case of the horizontal plane, for a better discernability.

Table 1

CLOSED ORBIT ANALYSIS WITH SEXTUPOLES

TUNE SHIFTS AND BETA VARIATIONS

	HORIZONTAL		VERTICAL	
Distr.	DBETA/BETA	D-TUNE	DBETA/BETA	D-TUNE
1	-0.61080e+00	0.11678e+00	0.17343e+00	0.36227e-01
2	0.21213e+00	0.11024e+00	-0.10000e+01	-0.10000e+01
3	0.12634e+00	0.53150e-01	0.32545e+00	0.21784e-01
4	0.74651e-01	0.29184e-01	-0.10000e+01	-0.10000e+01
5	-0.10000e+01	-0.10000e+01	-0.10000e+01	-0.10000e+01
6	0.44044e+00	0.59466e-01	0.21207e+00	0.67815e-01
7	-0.75274e-01	0.31351e-02	0.83884e-02	-0.89551e-02
8	0.54885e-01	0.58652e-01	0.31767e+00	-0.60770e-01
9	-0.10000e+01	-0.10000e+01	-0.10000e+01	-0.10000e+01
10	0.32682e+00	0.27776e-01	-0.10000e+01	-0.10000e+01
11	-0.10000e+01	-0.10000e+01	-0.10000e+01	-0.10000e+01
12	0.79245e+00	0.10302e+00	0.10874e+01	0.18147e-01
13	0.26772e+00	0.66674e-01	0.12157e+01	0.31952e-02
14	-0.10000e+01	-0.10000e+01	-0.10000e+01	-0.10000e+01
15	-0.10000e+01	-0.10000e+01	0.98408e+00	0.36816e-01
16	0.15255e+01	0.11120e+00	-0.10000e+01	-0.10000e+01
17	0.34190e+00	0.75801e-02	-0.15200e-01	0.59675e-01
18	0.17660e+00	-0.12165e-01	-0.41959e+00	-0.11303e-01
19	-0.10000e+01	-0.10000e+01	0.20870e+00	-0.36469e-01
20	0.41621e+00	0.52842e-01	0.84593e+00	0.81115e-01
21	0.60671e+00	0.49663e-01	0.98606e+00	0.43429e-01
RMS:	0.56475e+00	0.70768e-01	0.69632e+00	0.45952e-01

Table 2

Random Seed	Iter. No.	Corrected Orbit Distortion Max.(mm)	RMS (mm)	Comment	Kick Strength (mrad) Max.	RMS
	1	6.150	2.015		0.12355	0.03075
-23	2	0.358	0.133	Good	0.11658	0.03089
	3	0.003	0.001		0.11625	0.03092
	1	-3.246	1.336		-0.17355	0.04743
17	2	-0.966	0.339	Good	0.15357	0.04412
	3	-0.006	0.002		0.15351	0.04412
	1	5.228	1.689		0.12248	0.03580
43	2	0.784	0.281	Good	-0.08124	0.03205
	3	-0.004	0.001		-0.08124	0.03208
	1	8.389	2.863		0.13484	0.04460
7	2	-2.245	0.742	Fair	0.13641	0.04224
	3	-0.046	0.015		0.13609	0.04227
	1	-11.324	3.884		0.10809	0.03640
25	2	2.803	0.948	Fair	-0.09056	0.03175
	3	-0.029	0.008		-0.09056	0.03161
	1	-25.296	8.099		0.19611	0.05392
-7	2	11.974	4.052	Poor	0.09209	0.02962
	3	-0.315	0.111		0.09209	0.02932
	1	-28.990	10.612		0.15719	0.04916
-54	2	15.876	5.866	Poor	-0.09022	0.03136
	3	-0.652	0.227		-0.09022	0.03040

The reader will notice that we have displayed both the orbit distortions and the kick strengths to an excessive number of significant digits. This has been done merely to show what the algorithm does and it in no way implies that we expect the orbit distortions to be observable to such high accuracy.

Table 3

TABLE OF KICK STRENGTHS (milliradians). HORIZONTAL PLANE

MON. NUM.	MAGNET NUM.	ITER. NUMBER: 1	2	3	4	5
1	6	0.042472	0.076945	0.046834	0.042339	0.042335
2	34	0.112830	-0.004767	-0.005301	-0.005304	-0.005308
3	62	0.037541	0.059505	0.049341	0.045199	0.045197
4	90	0.138669	0.012961	0.010967	0.011046	0.011043
5	118	-0.023418	0.005356	-0.026847	-0.031044	-0.031050
6	146	0.076070	-0.028085	-0.029744	-0.030097	-0.030098
7	173	0.036559	0.023843	0.022304	0.022606	0.022607
8	185	0.027164	0.027164	0.027164	0.027164	0.027164
9	205	0.022299	0.022299	0.022299	0.022299	0.022299
10	217	0.003942	0.003942	0.003942	0.003942	0.003942
11	229	-0.026121	-0.026121	-0.026121	-0.026121	-0.026121
12	271	-0.008038	-0.008038	-0.008038	-0.008038	-0.008038
13	283	0.013105	0.013105	0.013105	0.013105	0.013105
14	299	-0.020396	-0.020396	-0.020396	-0.020396	-0.020396
15	315	-0.018751	-0.018751	-0.018751	-0.018751	-0.018751
16	333	0.009413	-0.025828	-0.032798	-0.035617	-0.035617
17	361	0.077437	-0.008263	-0.010680	-0.011295	-0.011300
18	389	0.069349	0.077276	0.058949	0.055566	0.055564
19	417	0.127981	0.022859	0.021157	0.020951	0.020949
20	445	-0.003765	-0.009032	-0.017066	-0.020455	-0.020456
21	473	0.125491	0.006630	0.005244	0.005070	0.005063
22	501	-0.046165	-0.025401	-0.045802	-0.049341	-0.049342
23	529	0.046987	-0.060338	-0.061279	-0.061321	-0.061325
24	557	-0.017000	-0.004707	-0.013266	-0.016718	-0.016720
25	585	0.157191	0.036337	0.035051	0.035147	0.035142

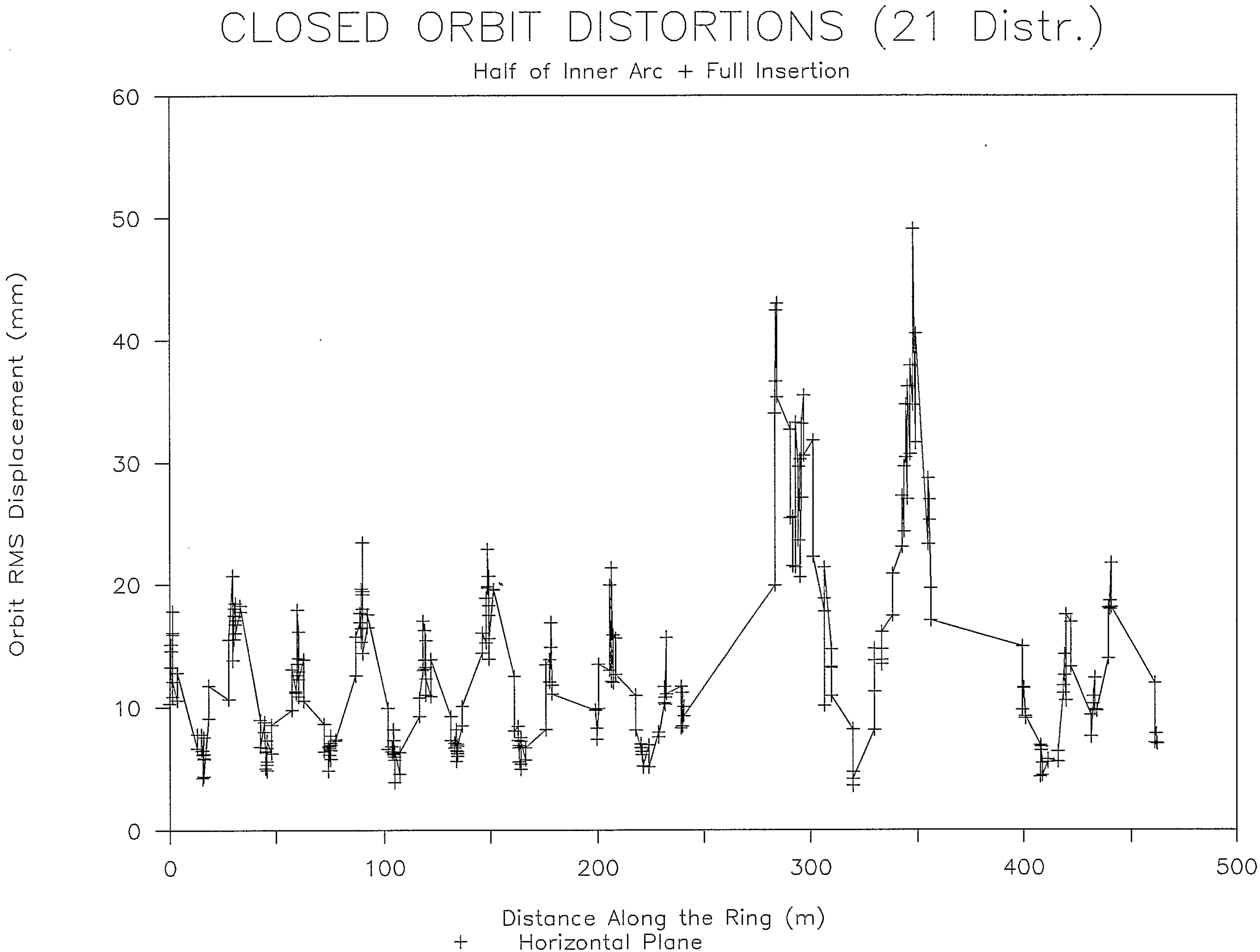

CLOSED ORBIT DISTORTIONS (21 Distr.)
Half of Inner Arc + Full Insertion
Orbit RMS Displacement (mm)
0
10
20
30
40
50
60
0
100
200
300
400
500
Distance Along the Ring (m)
+ Horizontal Plane

Figure 1

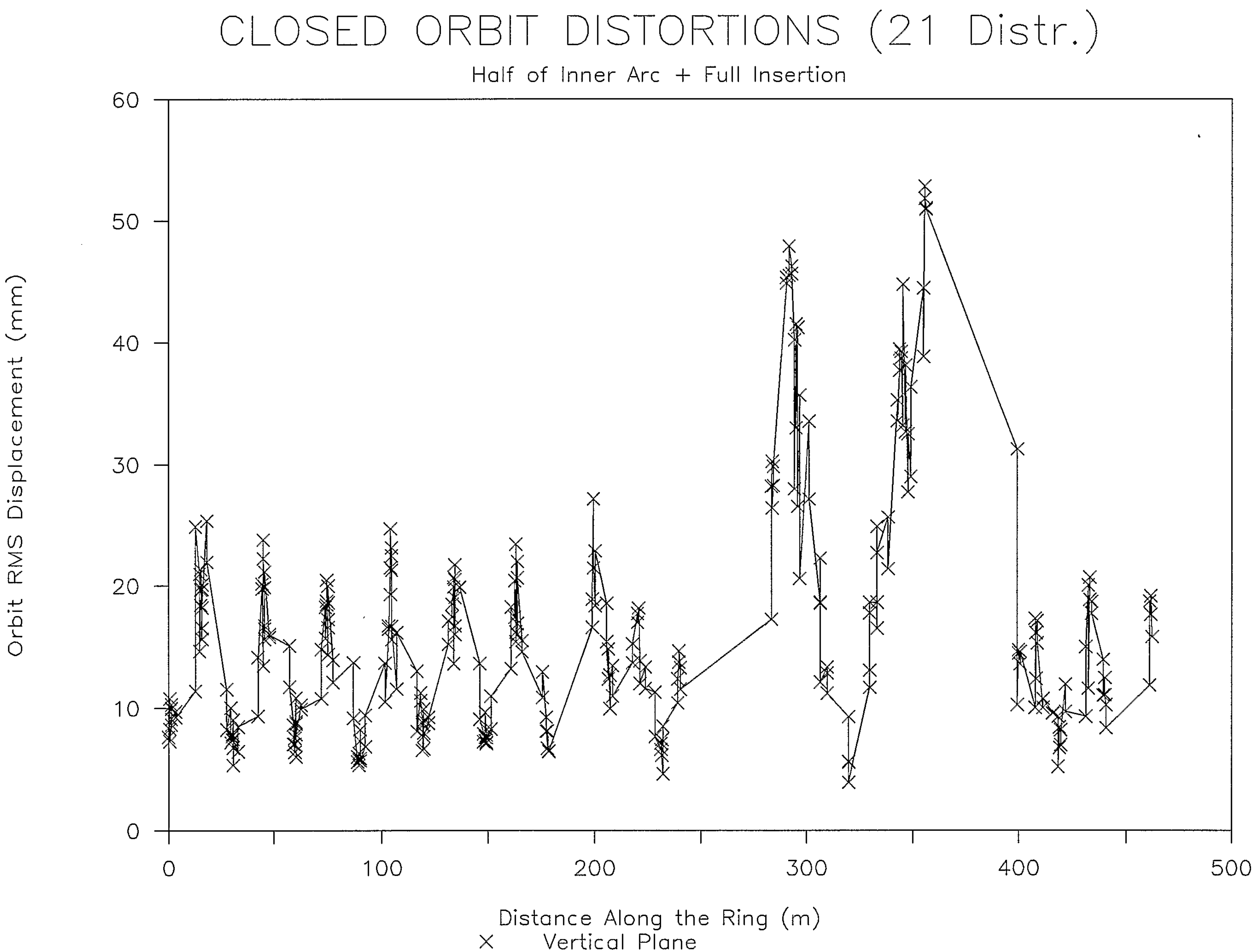

CLOSED ORBIT DISTORTIONS (21 Distr.)
Half of Inner Arc + Full Insertion
Orbit RMS Displacement (mm)
0
10
20
30
40
50
60
0
100
200
300
400
500
Distance Along the Ring (m)
Vertical Plane

Figure 2

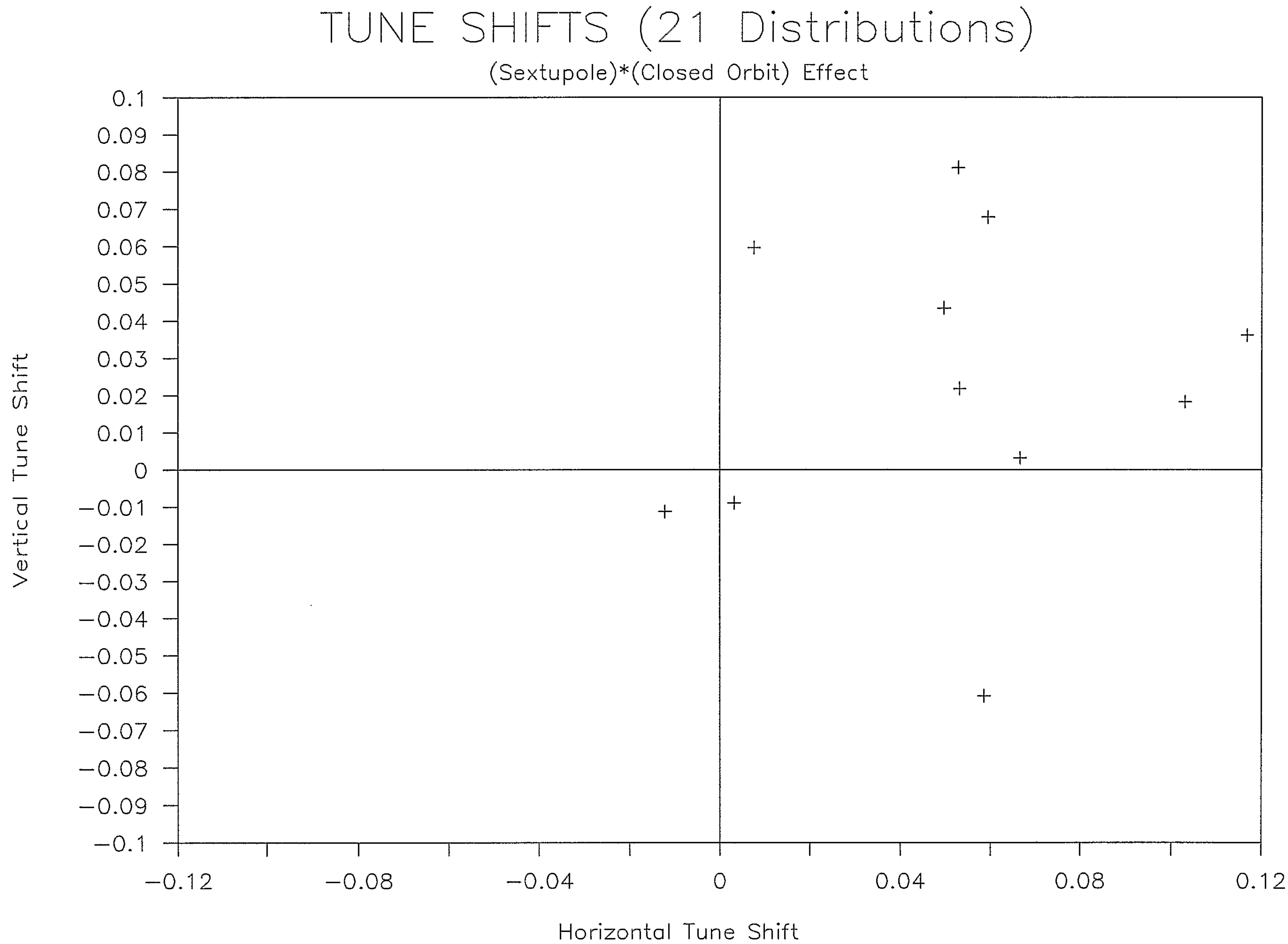
TUNE SHIFTS (21 Distributions)
(Sextupole)*(Closed Orbit) Effect
Vertical Tune Shift
Horizontal Tune Shift
0.1
0.09
0.08
0.07
0.06
0.05
0.04
0.03
0.02
0.01
0
−0.01
−0.02
−0.03
−0.04
−0.05
−0.06
−0.07
−0.08
−0.09
−0.1
−0.12
−0.08
−0.04
0
0.04
0.08
0.12

Figure 3

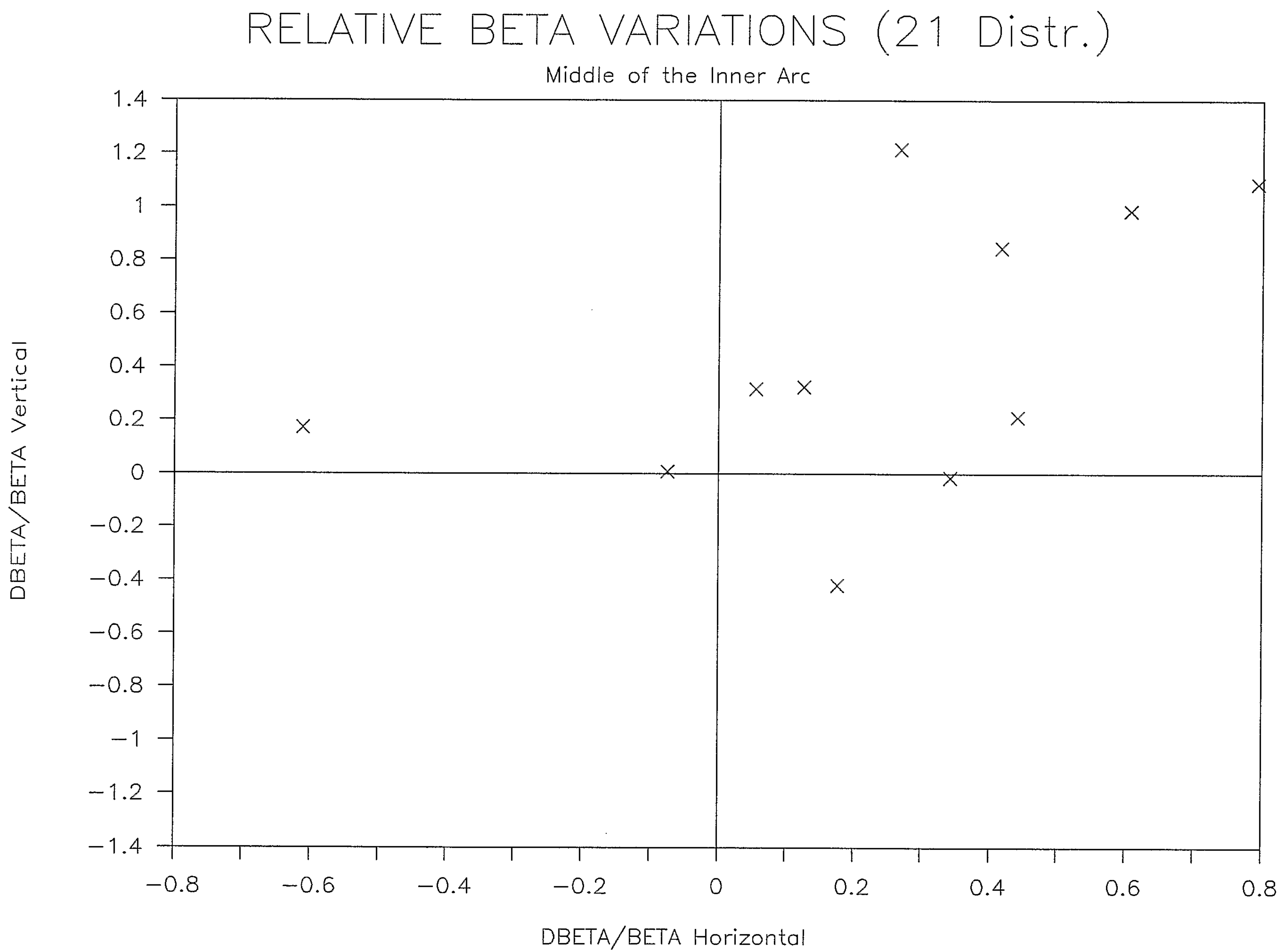
RELATIVE BETA VARIATIONS (21 Distr.)
Middle of the Inner Arc
DBETA/BETA Vertical
DBETA/BETA Horizontal
1.4
1.2
1
0.8
0.6
0.4
0.2
0
−0.2
−0.4
−0.6
−0.8
−1
−1.2
−1.4
−0.8
−0.6
−0.4
−0.2
0
0.2
0.4
0.6
0.8

Figure 4

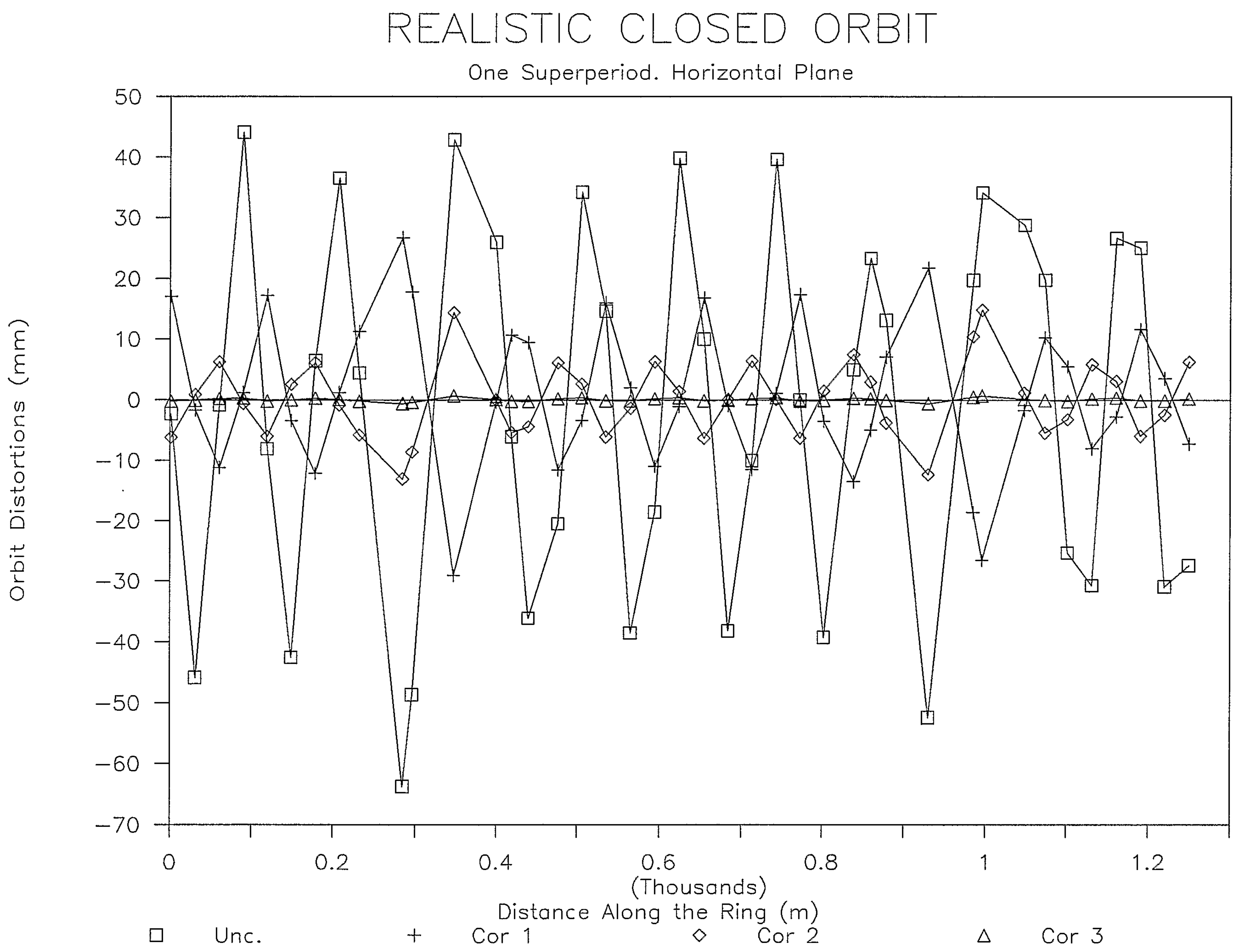

REALISTIC CLOSED ORBIT
One Superperiod. Horizontal Plane
Orbit Distortions (mm)
50
40
30
20
10
0
−10
−20
−30
−40
−50
−60
−70
0
0.2
0.4
0.6
0.8
1
1.2
(Thousands)
Distance Along the Ring (m)
Unc.
Cor 1
Cor 2
Cor 3

Figure 5

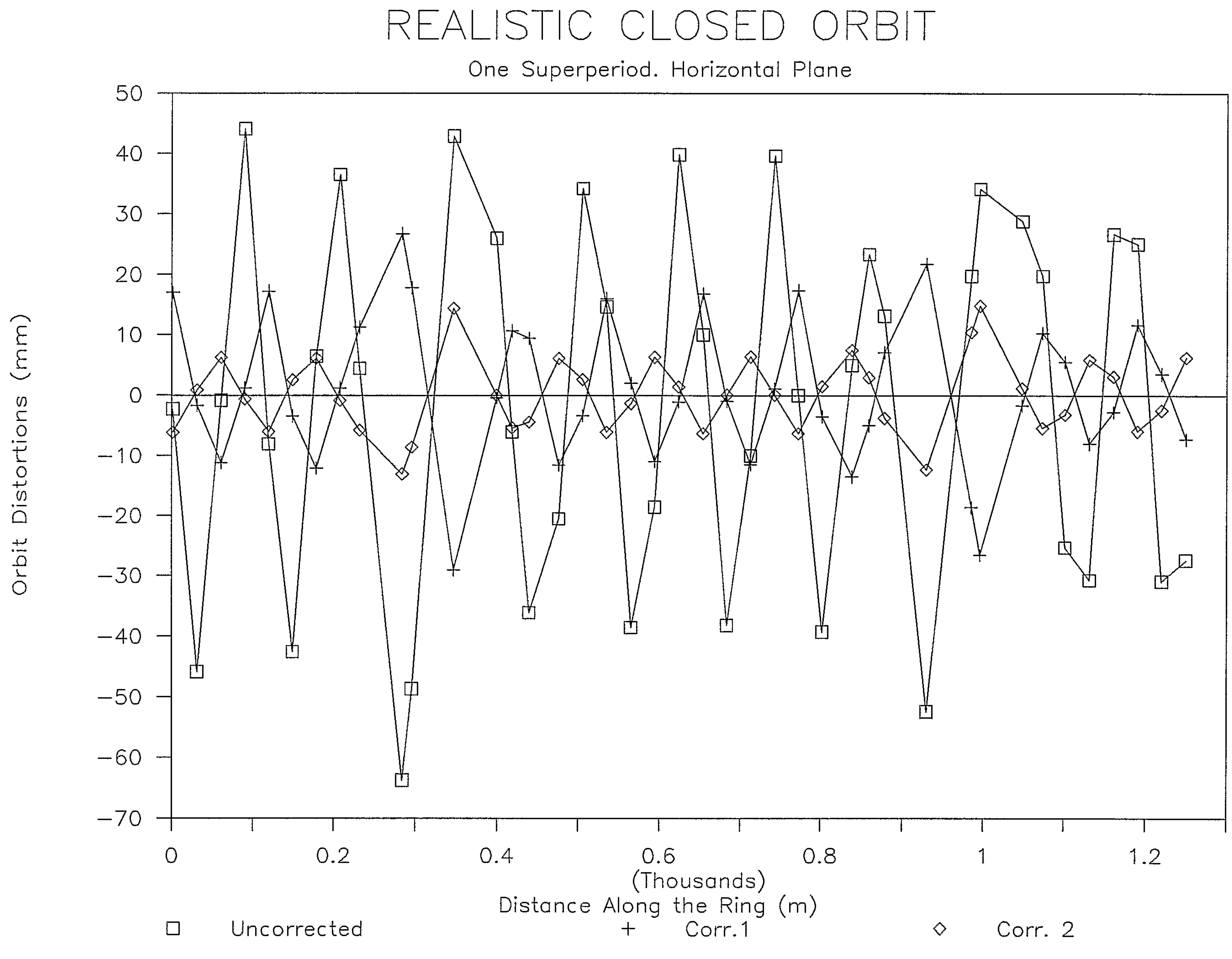
REALISTIC CLOSED ORBIT
One Superperiod. Horizontal Plane
Orbit Distortions (mm)
50
40
30
20
10
0
−10
−20
−30
−40
−50
−60
−70
0
0.2
0.4
0.6
0.8
1
1.2
(Thousands)
Distance Along the Ring (m)
Uncorrected
Corr.1
Corr. 2

Figure 5a

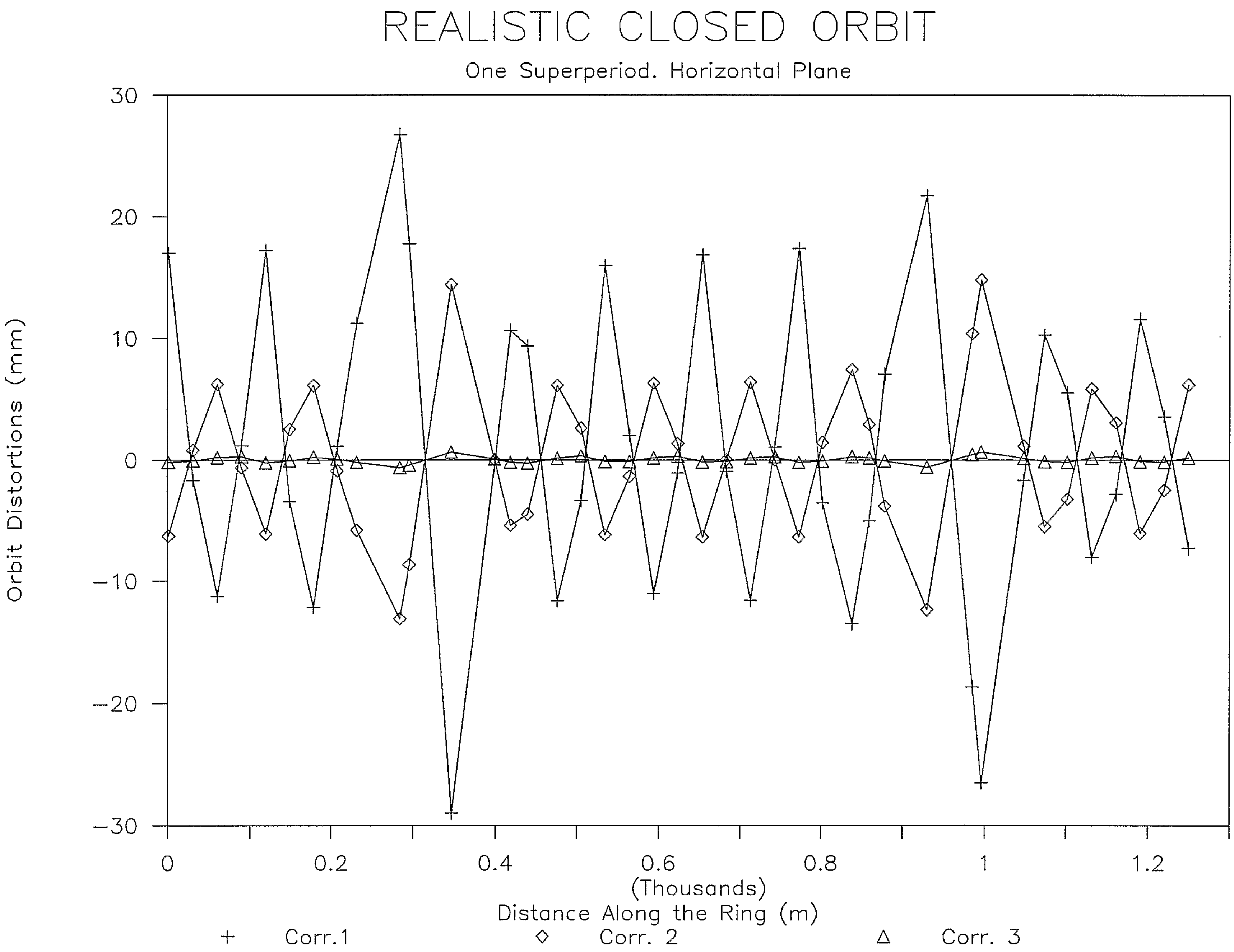
REALISTIC CLOSED ORBIT
One Superperiod. Horizontal Plane
Orbit Distortions (mm)
30
20
10
0
−10
−20
−30
0
0.2
0.4
0.6
0.8
1
1.2
(Thousands)
Distance Along the Ring (m)
Corr.1
Corr. 2
Corr. 3

Figure 5b

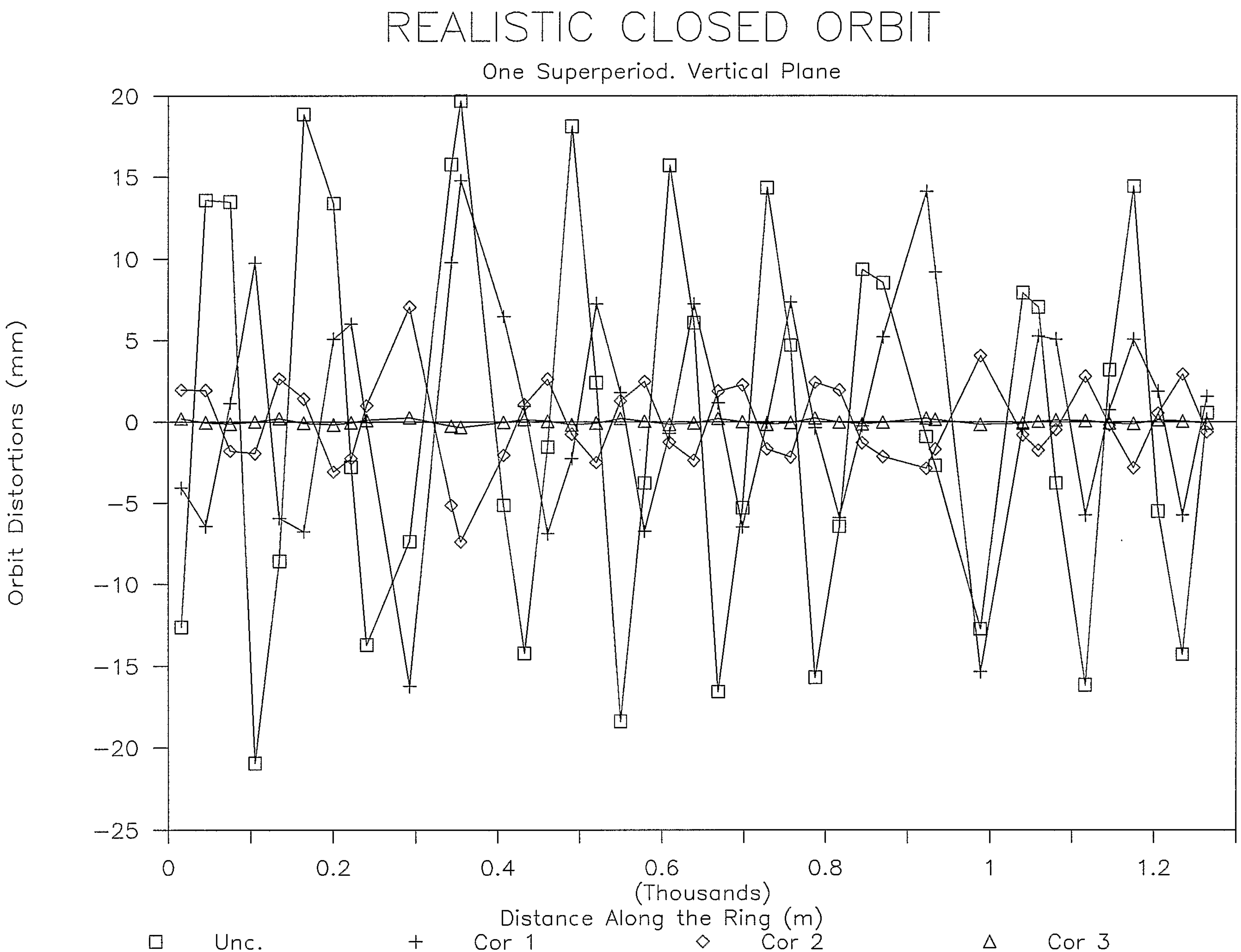
REALISTIC CLOSED ORBIT
One Superperiod. Vertical Plane
Orbit Distortions (mm)
20
15
10
5
0
−5
−10
−15
−20
−25
0
0.2
0.4
0.6
0.8
1
1.2
(Thousands)
Distance Along the Ring (m)
Unc.
Cor 1
Cor 2
Cor 3

Figure 6

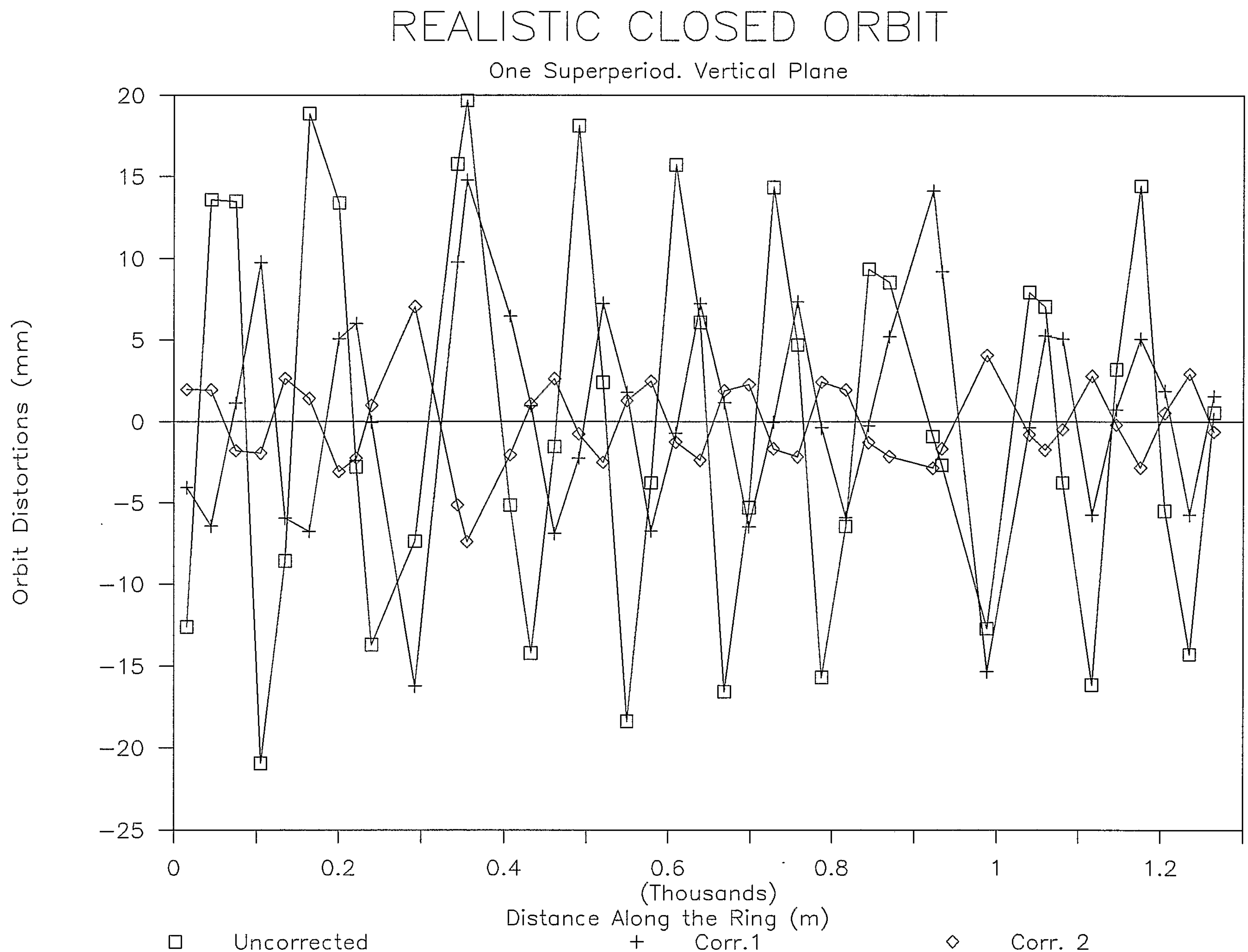
REALISTIC CLOSED ORBIT
One Superperiod. Vertical Plane
Orbit Distortions (mm)
20
15
10
5
0
−5
−10
−15
−20
−25
0
0.2
0.4
0.6
0.8
1
1.2
(Thousands)
Distance Along the Ring (m)
Uncorrected
Corr.1
Corr. 2

Figure 6a

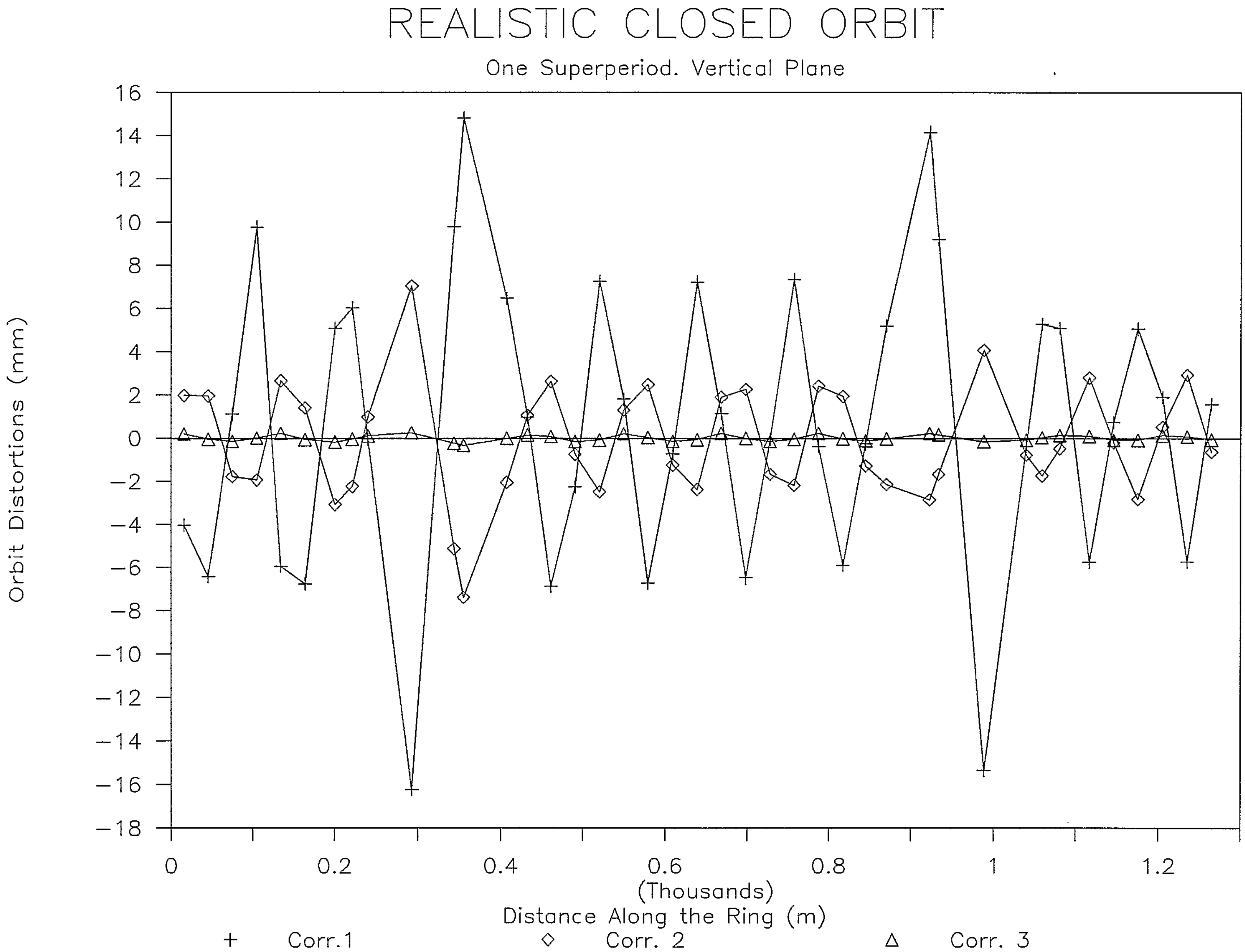

REALISTIC CLOSED ORBIT
One Superperiod. Vertical Plane
Orbit Distortions (mm)
16
14
12
10
8
6
4
2
0
−2
−4
−6
−8
−10
−12
−14
−16
−18
0
0.2
0.4
0.6
0.8
1
1.2
(Thousands)
Distance Along the Ring (m)
+ Corr.1
◇ Corr. 2
△ Corr. 3

Figure 6b